ResearchGate

See discussions, stats, and author profiles for this publication at: https://www.researchgate.net/publication/357987730

Cerebral Phospho-Tau Acts Synergistically with Soluble Aβ42 Leading to Mild Cognitive Impairment in AAV-AD Rats

Article *in* The Journal of Prevention of Alzheimer s Disease · July 2022

DOI: 10.14283/jpad.2022.18

CITATIONS
8

READS
158

10 authors, including:

Benoit Souchet
AgenT
40 PUBLICATIONS **847** CITATIONS
SEE PROFILE

Mickael Audrain
Air Liquide
102 PUBLICATIONS **1,587** CITATIONS
SEE PROFILE

Mattias Lindberg
Perha Pharmaceuticals
51 PUBLICATIONS **843** CITATIONS
SEE PROFILE

Orefice Nicola Salvatore
25 PUBLICATIONS **248** CITATIONS
SEE PROFILE

All content following this page was uploaded by Jérôme Braudeau on 01 February 2022.

The user has requested enhancement of the downloaded file.

J Prev Alz Dis 2022;
Published online January 25, 2022, http://dx.doi.org/10.14283/jpad.2022.18

Original Research

© Serdi and Springer Nature Switzerland AG 2022

Cerebral Phospho-Tau Acts Synergistically with Soluble Aβ42 Leading to Mild Cognitive Impairment in AAV-AD Rats

B. Souchet[1,2,3,7], M. Audrain[1,2,3], Y. Gu[4], M.F. Lindberg[5], N.S. Orefice[1,2,3], E. Rey[1,2,3], N. Cartier[1,2,3,6,], N. Janel[4,*], L. Meijer[5,*], J. Braudeau[1,2,3,7]*

1. INSERM UMR1169, Université Paris-Saclay, Orsay 94100, France; 2. CEA, DRF, Institut Jacques Monod, MIRCen, Fontenay-aux-Roses 92265, France; 3. Université Paris Saclay, Paris, France; 4. Université de Paris, BFA, UMR 8251, CNRS, F-75013 Paris, France; 5. Perha Pharmaceuticals, Presqu'île de Perharidy, Hôtel de recherche, 29680 Roscoff, France; 6. Present address Paris brain Institute (ICM), INSERM UMR1127, Paris Sorbonne Université, France; 7. AgenT, 4 rue Pierre Fontaine, Evry, France;
* These authors contributed equally to this work.

Corresponding Author: Jérôme Braudeau, AgenT SAS, Evry 91000, France, jerome.braudeau@agent-biotech.com

Abstract

BACKGROUND: Alzheimer's disease (AD) is a continuum of events beginning with an increase in brain soluble Aβ42 followed by the appearance of hyperphosphorylated tau (P-tau, asymptomatic stage). Mild Cognitive Impairment (MCI) then appears (prodromal stage). However, the individual contribution of these two soluble proteins in the onset of the first cognitive symptoms remains unclear.

OBJECTIVES: We sought to understand the specific impact of p-tau on the development of MCI in the AAV-AD rat model, a model of late-onset Alzheimer's disease (LOAD) predementia.

METHODS: We specifically reduced the phosphorylation level of tau while leaving Aβ42 levels unchanged using a DYRK1A protein kinase inhibitor, Leucettine L41, in an adeno-associated virus-based Alzheimer's disease (AAV-AD) rat model. Leucettine L41 was administered by intraperitoneal injection at 20 mg/kg per day in AAV-AD rats from 9 (late asymptomatic phase) to 10 (prodromal phase) months of age.

RESULTS: Decreased soluble forms of P-tau induced by chronic administration of Leucettine L41 did not change soluble Aβ42 levels but prevented MCI onset in 10-month-old AAV-AD rats.

CONCLUSIONS: The present study argues that P-tau is required to induce the development of MCI. Consistent with our previous findings that soluble Aβ42 is also required for MCI onset, the data obtained in the AAV-AD rat model confirm that the transition from the asymptomatic to the prodromal stage may be caused by the combined presence of both soluble brain forms of Aβ42 and p-tau, suggesting that the development of MCI may be the consequence of their synergistic action.

Key words: Hyperphosphorylated tau, Aβ42, mild cognitive impairment, AAV-AD rat, DYRK1A, leucettine.

Introduction

Alzheimer's disease (AD) is a major cause of dementia in which amyloid plaques and neurofibrillary tangles (NFTs) represent the main neuropathological hallmarks (1). Extracellular amyloid plaques are mainly formed by the aggregation of amyloid peptides (Aβ40 and Aβ42) whose production and accumulation are key elements in AD development (2). Intracellular NFTs are composed of aggregated hyper- and abnormal phosphorylated tau (P-tau) proteins (3).

In the past decades, substantial progress has been achieved in the field of AD describing the disease as a continuum of events (4). Thus, AD can be defined as the succession of 4 phases: pre-pathological, asymptomatic, prodromal and finally, dementia. In the pre-pathological stage, brain concentrations of soluble Aβ42 and P-tau are normal and the disease has not yet started. In asymptomatic individuals, when the disease begins, brain levels of Aβ42 (and potentially P-tau) slowly begin to rise. At this stage, CSF biomarkers are always negative (5). In the prodromal stage (or mild cognitive impairment due to AD), patients develop the first cognitive symptoms due to the toxicity of amyloids (and potentially of P-tau) (6 , 7) and are in the transition phase for CSF biomarkers. Thus, although the increase in CSF Aβ42 and P-tau may begin early, the threshold for positivity of both amyloid and tau markers is certainly not reached until late MCI or dementia in most cases (8). The asymptomatic and prodromal phases constitute the predementia stage of Late Onset AD (LOAD) where cognitive symptoms are defined by a Clinical Dementia Rating (CDR) score ≤ 0.5 (9). Patients subsequently develop dementia. At this stage, almost all, if not all, demented patients are positive for CSF (Aβ42 and P-tau) and Positron Emission Tomography (PET) (senile plaques and tangles) biomarkers (8).

At the prodromal stage, only a small number of patients are thereby positive for PET or CSF biomarkers (8) suggesting that the molecular inducers of MCI are more likely to be the soluble forms than the aggregated forms (10, 11). No publication describes a method for *in situ* determination of either cerebral soluble amyloid peptide or P-tau concentration during the patient's lifetime. The absence of such a dosing greatly limits the possibility to assess the involvement of these two soluble markers during prodromal stage establishment and earlier. An essential question therefore remains unanswered: what is responsible for the appearance of these first cognitive impairments: soluble Aβ42, soluble

Received November 17, 2021
Accepted for publication December 5, 2021

hyper-phosphorylated tau or a synergetic combination of both?

To investigate this question, we used an adeno-associated virus-based Alzheimer's disease (AAV-AD) rat model (12). By contrast to transgenic models, the AAV-AD model is based on the induction of mosaicism and aneuploidy of the human and mutated APP gene in the hippocampus through gene transfer, thus mimicking one of the suspected non-congenital aetiologies of LOAD (12-14). AAV-based gene transfer was performed in 2-month-old adult animals. AAV-AD rats thus mimic the pre-dementia progression of LOAD by including at least its pre-pathological, asymptomatic and prodromal phases (15). Interestingly, MCI appears only when both soluble amyloid peptide and P-tau are present, suggesting that their combined presence is necessary to initiate cognitive decline (12).

We previously described that avoiding Aβ42 production by rebalancing non-amyloidogenic/amyloidogenic pathways in AAV-AD rats prevents the development of MCI even if the levels of hyperphosphorylated tau are maintained (15). The presence of soluble forms of Aβ42 in the brain thus appears to be necessary for the development of MCI. However, the involvement of P-tau in MCI onset was yet unknown. The objective of the present study was therefore to understand the specific impact of tau hyperphosphorylation on MCI onset. Since an increase in the level of DYRK1A protein, a tau kinase (16), was observed in AAV-AD rats at 10 months of age (prodromal stage)(12), we chose to target this kinase via a pharmacological drug, Leucettine L41, to specifically reduce P-tau levels. While Leucettine L41 exerts an inhibitory activity on DYRK1A kinase (17, 18), it has been shown to decrease tau hyperphosphorylation in vitro (19) without acting on brain soluble Aβ42 production *in vivo* (20). Here, we described that Leucettine L41 reduced cerebral P-tau brain concentrations resulting in the prevention of MCI onset, despite unchanged and elevated Aβ42 concentrations. With our previous report (12), our data indicate that the presence of both soluble Aβ42 and P-tau are necessary for MCI onset.

Methods

Cellular assays with Leucettine L41

NanoBRET target engagement intracellular kinase Assay

The nanoLuc-DYRK1A fusion expression vector (Promega) was transfected into HEK-293T cell at a density of $2x10^5$ cells/mL using FuGENE HD (Promega), according to the manufacturer's protocol. Cells were grown for 24 hours at 37°C, 5% CO2, then were washed and re-suspended in OptiMEM medium. For the BRET assay, $1.7x10^4$ cells/well were plated in a white 96-well plate (Greiner). Various concentrations of Leucettine L41 and the BRET-assay tracer K9 (Promega, 0.5 μM final concentration) were added to the cells, which were then incubated for an additional 2 hours. Finally, the NanoGlo substrate and extracellular NanoLuc inhibitor (Promega) were added into the supernatant prior to luminescence (450-480 nm, 0.5 s integration time, donor) and fluorescence (610 nm, monochromator settings, acceptor) measurements using BMG CLARIOStar. The IC50 calculation was performed using SigmaPlot software, as described previously (21).

Culture and treatment of cell lines

SH-SY5Y-4R-tau neuroblastoma cells overexpressing the four-repeat (4R) tau isoform were cultured in Dulbecco's Modified Eagle Medium (DMEM): Nutrient Mixture F-12 (DMEM/F-12, Gibco, c/o Invitrogen, Saint Aubin, France) containing 1% Penicillin Streptomycin mixture (Gibco) and 10% fetal bovine serum (FBS, Gibco) in a humidified, 5% CO2 incubator at 37°C. Twenty-four hours after seeding $7.5x10^5$ cells into 60 mm dishes, Leucettine L41 was added at 10 or 30 μM (with a final concentration of 0.1% DMSO) and incubated with the cells for 6 h. Cells were scrapped in cold PBS, centrifuged at 10,000 rpm for 1 min at 4°C, and pellets were snap-frozen in liquid nitrogen.

Cell lysis, electrophoresis and Western Blotting

Cell pellets were lysed on ice in PY buffer [25 mM MOPS (Sigma), 15 mM EGTA (Sigma), 15 mM Magnesium chloride (MgCl2, Sigma), 60 mM β-glycerophosphate (Sigma), 15 mM p-nitrophenylphosphate (Sigma), 2 mM DL-dithiothreitol (DTT, Sigma), 1 mM sodium orthovanadate (Sigma), 1 mM sodium fluoride (Sigma), 1 mM di-sodium phenylphosphate (Sigma), protease inhibitor cocktail (Complete, Roche), pH 7,2] supplemented with 0.1% Nonidet P-40, and then centrifuged (17,000 g for 1 min at 4 °C). Protein extracts were mixed (1:1 v/v) with sample buffer (2x NuPAGE LDS sample buffer, 200 mM DTT). Following heat denaturation, 20 μg of proteins were loaded on NuPAGE precast 4–12% Bis-Tris protein gels (ThermoFisher). Electrophoresis was run in MOPS buffer. Rapid blot transfers were performed at 2.5 A/25 V for 7 min. Membranes were blocked in milk (5% Regilait in Tris Buffered Saline with 0.1% Tween (TBST)) for 1 h and then incubated with the antibodies against phospho T^{212}-tau (Abcam, 1/2,000 in milk, overnight at 4°C), total tau (tau-5, Abcam, 1/2,000 in milk, overnight at 4°C), or GAPDH (BioRad, 2 h at RT, 1/30,000). Finally, membranes were incubated for 1 h at RT with goat anti-rabbit or goat anti-mouse antibodies (BioRad), and chemiluminescent detection was achieved with homemade ECL-Tris buffer (100 mM Tris pH 8.5, 0.009% H2O2, 0.225 mM p-coumaric acid, 1.25 mM luminol) with Fusion Fx7 camera software.

Animals

Male Wistar rats (eight-week-old; SARL JanvierLabs, Le Genest Saint Isle, France) were used in this study. All experiments were conducted in accordance with the ethical standards of French and European regulations (European Communities Council Directive 2010/63/EU, authorization number APAFIS#4449-2016031012491697).

AAV-AD induction

Rats were anesthetized by an intraperitoneal injection of ketamine/xylazine and placed in a stereotactic frame (Stoelting, Wood Dale, IL, USA). Stereotactic intracerebral injections of AAVs into the hippocampi of both hemispheres were performed, using the following coordinates: antero-posterior: -3.6 mm, lateral: ± 2.5 mm, ventral: -3.3 mm relative to bregma. A volume of 4 μL of viral preparation was injected into each site ($2.5x10^{10}$ vg/site and $5x10^{10}$ vg/site for PS1 and APP, respectively) at a rate of 0.25 μL/minute. Two groups of animals were produced. Control animals were induced by intra-hippocampal injection of the virus encoding the human $PS1_{M146L}$ gene only (AAV-CAG-$PS1_{M146L}$). AAV-AD animals were induced by intra-hippocampal injection of both viruses encoding the human $PS1_{M146L}$ gene and the human APPSL gene (and AAV-CAG-APP_{SL} + AAV-CAG-$PS1_{M146L}$) (12). Thus, the AAV-AD model results in increased copy number of the APP gene with Swedish-London mutations compared to control animal, and genetic changes are restricted to a limited number of hippocampal neurons. This thus mimics a suspected etiology of LOAD: somatic neo-mutations (mosaicism) (13) and APP gene duplications (aneuploidy) (14) appearing only from adulthood.

Leucettine L41 treatment

The pre-weighed compound was dissolved in DMSO/PEG300/water (5/35/60) to a final concentration of 2 mg/mL for a dosing at 20 mg/kg. The formulation was prepared on the day of the *in vivo* experiment. Rats received five intraperitoneal injections per week for five weeks. Controls rats and vehicle-treated AAV-AD rats were treated with vehicle only (dissolution solvent).

Tissue collection and sample preparation

Rats were anesthetized with ketamine/xylazine and were first placed in a stereotactic frame to collect CSF by puncturing the cisterna magna with a low dead space syringe. The right brain was dissected to isolate the hippocampus for biochemistry while the entire left brain was preserved for immunochemistry. Samples were homogenized in a lysis buffer (150 mM NaCl and 1% Triton in Tris-buffered saline) containing phosphatase (Pierce) and protease (Roche) inhibitors and centrifuged for 20 min at 15000 x g for biochemistry analysis.

ELISA

Soluble Aβ was quantified using the triplex Aβ Peptide Panel 1 (6E10) V-PLEX Kit (Meso Scale Diagnostics, Rockville, USA). Hyperphosphorylated tau was quantified using the Innogenetics Phospho-tau 181P kit (Fujirebio Europe, Ghent, Belgium). The ELISA was performed according to the kit manufacturer's instructions in each case.

Western blotting

Equal amounts of protein (30 μg) were separated by electrophoresis in NuPAGE Bis-Tris Gels (Life Technologies) and transferred to nitrocellulose membranes. The membranes were hybridized with various primary antibodies: APP 6E10 (1/500, Covance), PS1 (1/1000, Millipore), APP C-ter (1/500, Millipore), P-tau Thr422 (1/1000, Invitrogen), P-tau Thr212 (1/1000, Invitrogen), GAPDH (1/1000, Abcam). Various secondary antibodies were also used: ECL horseradish peroxidase linked anti-rabbit, ECL horseradish peroxidase linked anti- mouse, ECL horseradish peroxidase linked anti-rat (all 1/2000, GE Healthcare). Protein levels loaded were normalized by the intensity of GAPDH.

Immunohistochemistry and Image Acquisition

Cryosections were washed with 0.25% Triton X-100 in PBS and saturated by incubation (0.25% Triton in PBS/5% goat serum). They were then incubated with one or more of the following primary antibodies: APP C-ter, total APP (1/500, Millipore) and 6E10 (human APP, 1/500, Covance). Images were captured using a Leica TCS SP8 confocal microscope.

Behavioral assessment

Open-field. The apparatus consisted of an open-topped, opaque plexiglas box measuring 90 x 90 x 70 cm placed in a room with controlled dim lighting (40 lux) and constant white noise at 40 dB. Rats were placed in the center of the arena and a video recording was made over a period of five minutes. The behavior of the animals was analyzed from this video. The arena was divided into a central region and a peripheral region, and the time spent in the center and periphery of the open-field was measured.

Morris water maze. Experiments were performed in a 180 cm diameter / 50 cm deep tank, filled with opacified water kept at 21°C, and equipped with a 18 cm diameter platform, submerged 1 cm below the water surface. Visual clues were positioned around the pool and luminosity was maintained at 350 lux. Rats were initially exposed to a learning phase, which consisted of daily sessions (three trials per session) on five consecutive days. The starting position varied pseudo-randomly, between the

Figure 1. Leucettine L41 binds to DYRK1A and inhibits T212 tau-phosphorylation in cells

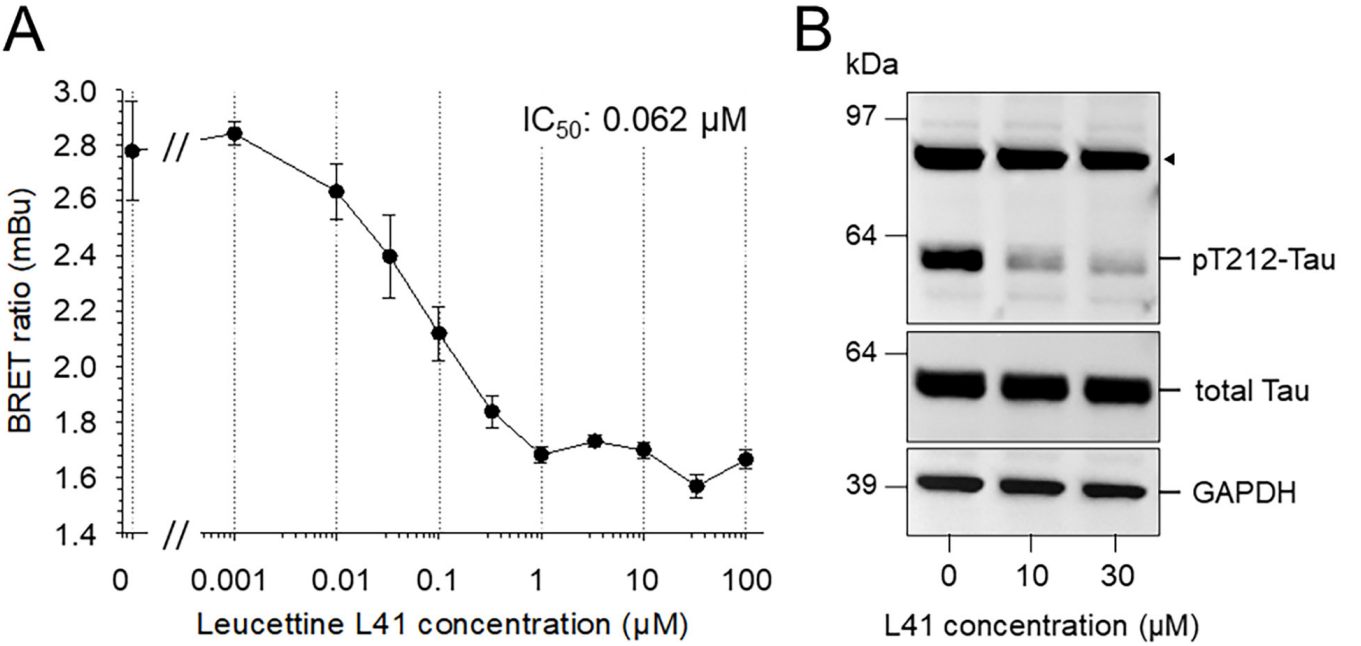

A. Leucettine L41 target engagement with DYRK1A was demonstrated in HEK293 cells expressing a DYRK1A-NanoLuc fusion protein. Two hours after adding the fluorescent tracer and increasing concentrations of L41 to HEK293 cells transiently transfected with a DYRK1A-NanoLuc fusion vector, NanoGlo substrate was added to the cells enabling light emission and bioluminescence resonance energy transfer (BRET). BRET ratios were calculated by dividing the tracer (acceptor) emission signal (610 nm) by the NanoLuc (donor) luminescence signal (450-480 nm) (results expressed in milliBRET units, mBu). L41 inhibits BRET in a dose-dependent manner by hampering DYRK1A active site accessibility to the tracer. Individual data points are the mean ± SD of two technical replicates. Intracellular IC50 was calculated using SigmaPlot software. B. Inhibition of tau Thr212 phosphorylation by Leucettine L41. SH-SY5Y cells overexpressing the 4R tau isoform (SH-SY5Y-4R-tau) were treated for 6 h with 0 (0.01% DMSO), 10 or 30 μM Leucettine L41. Proteins were resolved by SDS-PAGE and analyzed by Western blotting with antibodies directed against pT212-Tau, total tau (tau-5) or glyceraldehyde-3-phosphate dehydrogenase (GAPDH) (used as loading control). Arrow indicates an unidentified protein which cross-reacts with pT212-tau antibodies and which constitutes an internal loading control.

four cardinal points. A mean interval of 20 min was set between trials. The trial was considered to have ended when the animal reached the platform. The memorization of the platform position by the animals was validated by a probe test (in which the platform was no longer available) carried out 4 hours after the last training trial to confirm the good memorization of platform position and thus intact learning capacities, intact learning abilities with a clear spatial bias. Accelerated forgetting was assessed 120 hours after the last training trial in a probe trial in which the platform was no longer available. Animals were monitored using EthoVision software.

Statistical analysis

Data are expressed as the mean ± SEM. Statistical analyses were performed using GraphPad Prism (GraphPad Soft- ware, La Jolla, CA, USA) and the statistical significance was set to a p-value < 0.05 for all tests. One-way ANOVA followed by Tukey's post-hoc test or two-way ANOVA followed by Holm-Šídák's post-hoc test were used to determine the significance of differences between groups. The ROUT method was used to identify outliers (Q=1%). Only one outlier has been excluded of the statistical analysis for the open-field test.

Results

Leucettine L41 binds to and inhibits DYRK1A activity, leading to a reduction of tau phosphorylation level in cells

We first intended to measure Leucettine L41 affinity for DYRK1A in cells using a NanoBRET (Bioluminescence resonance energy transfer) target engagement assay. This technique enables real-time measurement of ligand-protein interaction in living cells. It uses NanoLuc as bioluminescent donor, which provides resonance energy, and an acceptor (tracer) that emits fluorescence upon activation. In our case, HEK-293 cells were first transfected in order to express a DYRK1A-NanoLuc fusion protein. A maximal BRET signal was achieved by binding of the fluorescent tracer to the intracellular DYRK1A binding pocket, without addition of L41 (Fig. 1A). The binding of Leucettine L41 to DYRK1A results in a dose-dependent loss in BRET signal due to its competition with the tracer, showing an intracellular IC50 of 0.062 μM.

To confirm that Leucettine L41 binding to DYRK1A inhibits its catalytic activity in a cellular context, we made use of a SH-SY5Y neuroblastoma cell line overexpressing

Figure 2. Chronic treatment with Leucettine L41 does not affect AAV-AD induction

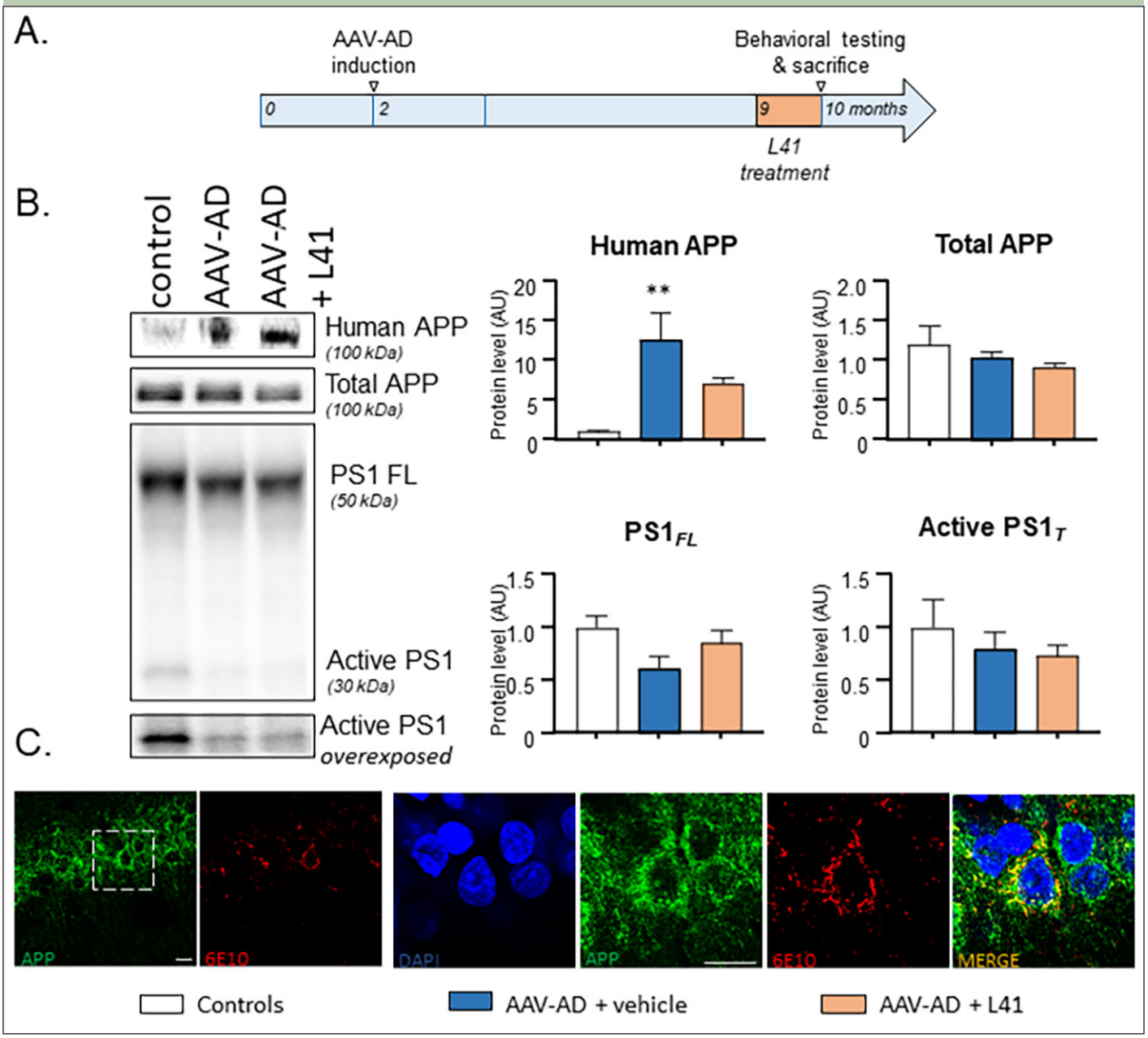

A. Schematic representation of the experimental timeline. B. Western blot experiments showing the expression of human APP (6E10 antibody), total APP (rat + human forms; APP C-ter antibody (22C11), PS1 FL (full length) and active PS1 (truncated) (12), confirming transgene expression one month after injection with or without Leucettine L41 treatment. C. Confocal microscopy acquisition performed in sections from AAV-AD hippocampus: human APP (red) was expressed in sparse neurons in CA2/CA3 layers (blue) harboring endogenous APP (green). Right panels described higher magnificence than left panels. Bars represent the mean ± SEM. Statistical analyses were performed using one-way ANOVA followed by Tukey's multiple comparisons post-hoc test. Significant differences between vehicle-treated control rats and vehicle or L41-treated AAV-AD rats are indicated by $^{**}p < 0.005$.

4R-tau isoform and analyzed the effects of L41 on the phosphorylation of Thr212-tau, a well-known DYRK1A phosphorylation site (16). SH-SY5Y-4R-tau cells were exposed to 10 or 30 μM of L41 for 6 h, then harvested and their proteins resolved by SDS-PAGE, followed by Western blotting with antibodies against P-Thr212-tau, total tau (tau-5) and GAPDH (loading control) (Fig. 1B). Results show a strong inhibition of tau phosphorylation at Thr212 at both 10 and 30 μM of L41, further confirming its specific effect on DYRK1A in cells.

Leucettine L41 administration does not prevent transgenes expression in AAV-AD rats

We first verified that the Leucettine L41 did not affect the gene transfer-mediated induction in the AAV-AD model. We administrated Leucettine L41 in 9-month-old AAV-AD rats, 1 month starting before prodromal stage onset, before tau hyperphosphorylation and MCI (12). Vehicle-treated control rats (n=10), vehicle-treated

Figure 3. Chronic treatment with Leucettine L41 reduces the levels of hyperphosphorylated tau without changing the amounts of soluble amyloid

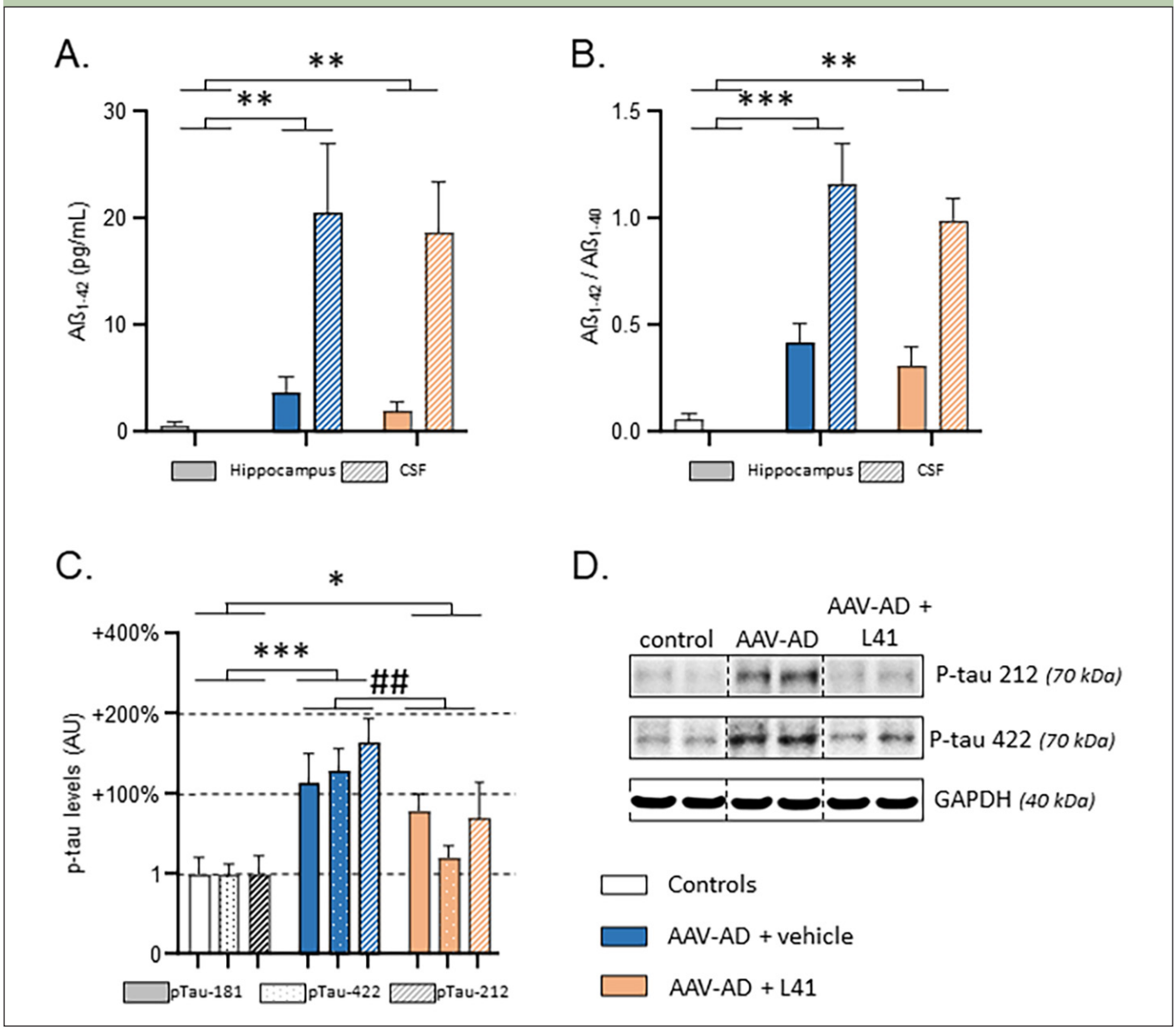

A. Comparative analysis of Aβ42 in hippocampus and CSF. B. Comparative analysis of Aβ42/Aβ40 ratio in hippocampus and CSF. C. Comparative analysis of phospho-Thr181, phospho-Thr422 and phospho-Ser212 assessed by ELISA or Western Blot in hippocampus. D. Western blot showing the expression of phospho-Thr212, phospho-Ser422 and GAPDH protein. Bars represent the mean ± SEM. Statistical analyses were performed using two-way ANOVA followed by Holm-Šídák's post-hoc test. Significant differences between vehicle-treated control rats and vehicle or L41-treated AAV-AD rats are indicated by *p <0.05, **p <0.005 and ***p <0.0005. Significant differences between vehicle-treated AAV-AD rats and L41-treated AAV-AD rats are indicated by ##p <0.005.

(n=12) and L41-treated AAV-AD rats (n=13) have been injected at 9 months (asymptomatic) using intraperitoneal procedure during 5 weeks (25 injections in total) and sacrificed at 10 months (prodromal) (Fig. 2A). We first evaluated whether L41 modified AAV-AD induction (Fig. 2B and C). Western blot analysis of whole hippocampus extracts revealed comparable endogenous APP, PS1 full-length ($PS1_{FL}$) and truncated PS1 N-terminal fragment ($PS1_{NTF}$) levels in control and AAV-AD rats. Human APP (detected with 6E10 antibody) was only present in AAV-AD rats (one-way ANOVA: $p = 0.005$; vehicle treated controls: 1.00 ± 0.15 AU; vehicle treated AAV-AD: 12.57 ± 3.40 AU; L41 treated AAV-AD: 7.07 ± 0.73 AU; Tukey's multiple comparisons post-hoc test: $p = 0.007$ and $p = 0.132$ respectively). Leucettine L41 treatment did not modify the levels of exogenous and endogenous APP as well as $PS1_{FL}$ and $PS1_{NTF}$ (Fig. 2B). By immunohistochemistry, we confirmed the presence of sparse neurons expressing exogenous human APP located in hippocampus in vehicle- and L41-treated AAV-AD rats (Fig. 2C). These findings confirm that L41 treatment did not affect AAV-AD induction.

Figure 4. Chronic treatment with Leucettine L41 does not reduce mild anxiety but prevents mild cognitive impairment in 10-month-old AAV-AD rats

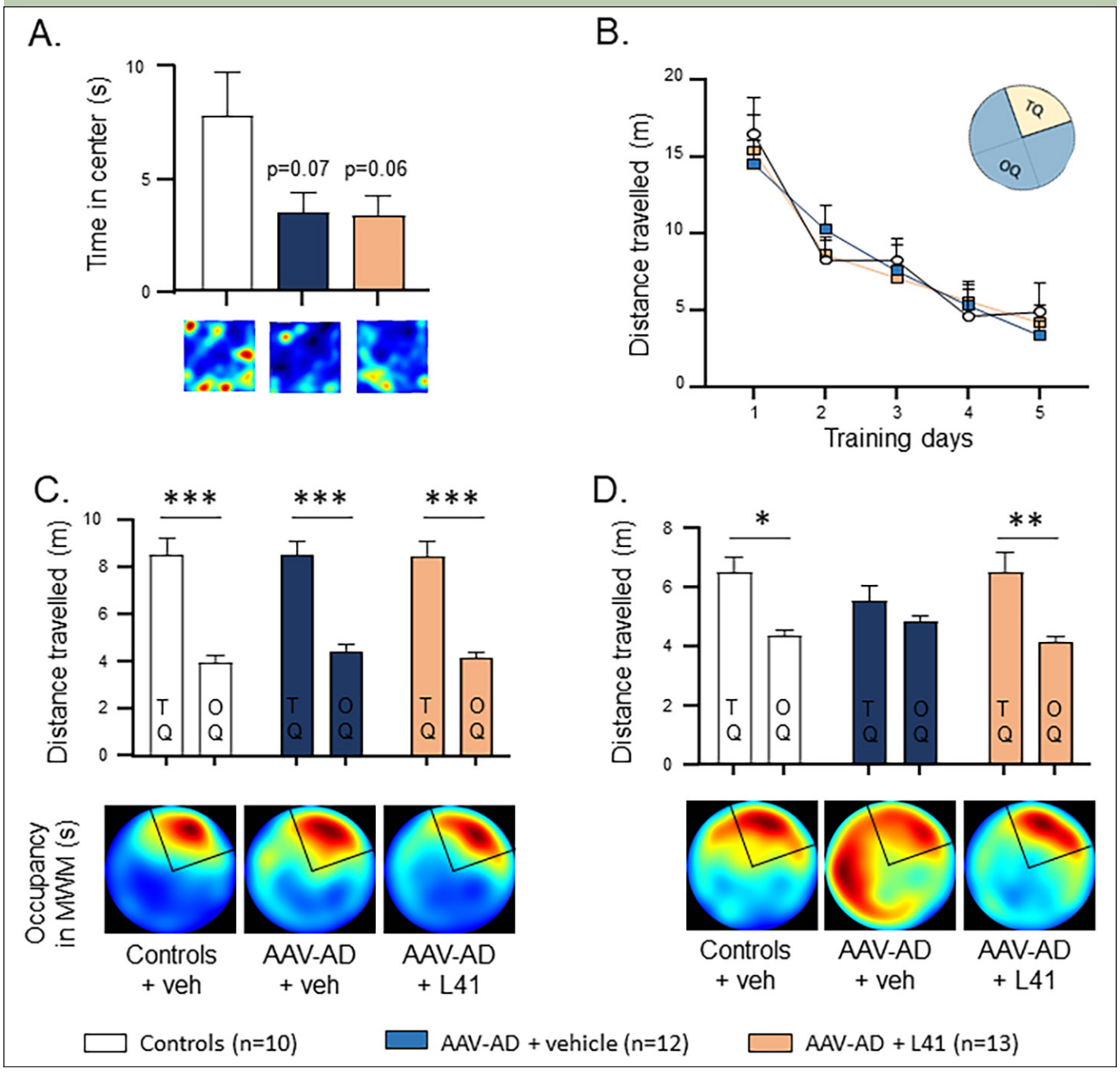

A. Time spent in the center of the open-field area. B. Learning curves representing the travelled distance during the 5 training days in the 4 quadrants (TQ = target quadrant that housed the platform during the training sessions, OQ = mean in the 3 other quadrants). C. Probe trial performance at 4 h after the last training session. D. Probe trial performance at 120 h after the last training session. For each figure, bottom group occupancy plots allow to visualize the mean areas in which the animals spent most time during the test. Bars represent the mean ± SEM. Statistical analyses were performed using one-way ANOVA followed by Tukey's post-hoc test or two-way ANOVA followed by Holm-Šídák's multiple comparisons post-hoc test. Significant differences are indicated by *P < 0.05, **P < 0.005 or ***P < 0.0005.

Leucettine L41 reduces hyperphosphorylated tau levels without affecting soluble Aβ production

Vehicle- or L41-treated AAV-AD rats showed higher concentrations of Aβ42 compared to vehicle-treated control rats in both hippocampus and CSF (two-way ANOVA, group effect: $p = 0.0021$. Holm-Šídák's multiple comparisons post-hoc test: $p = 0.003$ and $p = 0.007$, respectively; Fig. 3A). Similar findings were found for Aβ42/40 ratios (two-way ANOVA, Group effect: $p = 0.0001$. Holm-Šídák's multiple comparisons post-hoc test: $p < 0.001$ and $p = 0.002$, respectively; Fig. 3B). These results confirm that L41 treatment does not affect amyloid production in 10-month-old AAV-AD rats. As

Figure 5. The synergistic action of soluble Aβ42 and P-tau in the development of MCI is supported by AAV-AD rat investigation

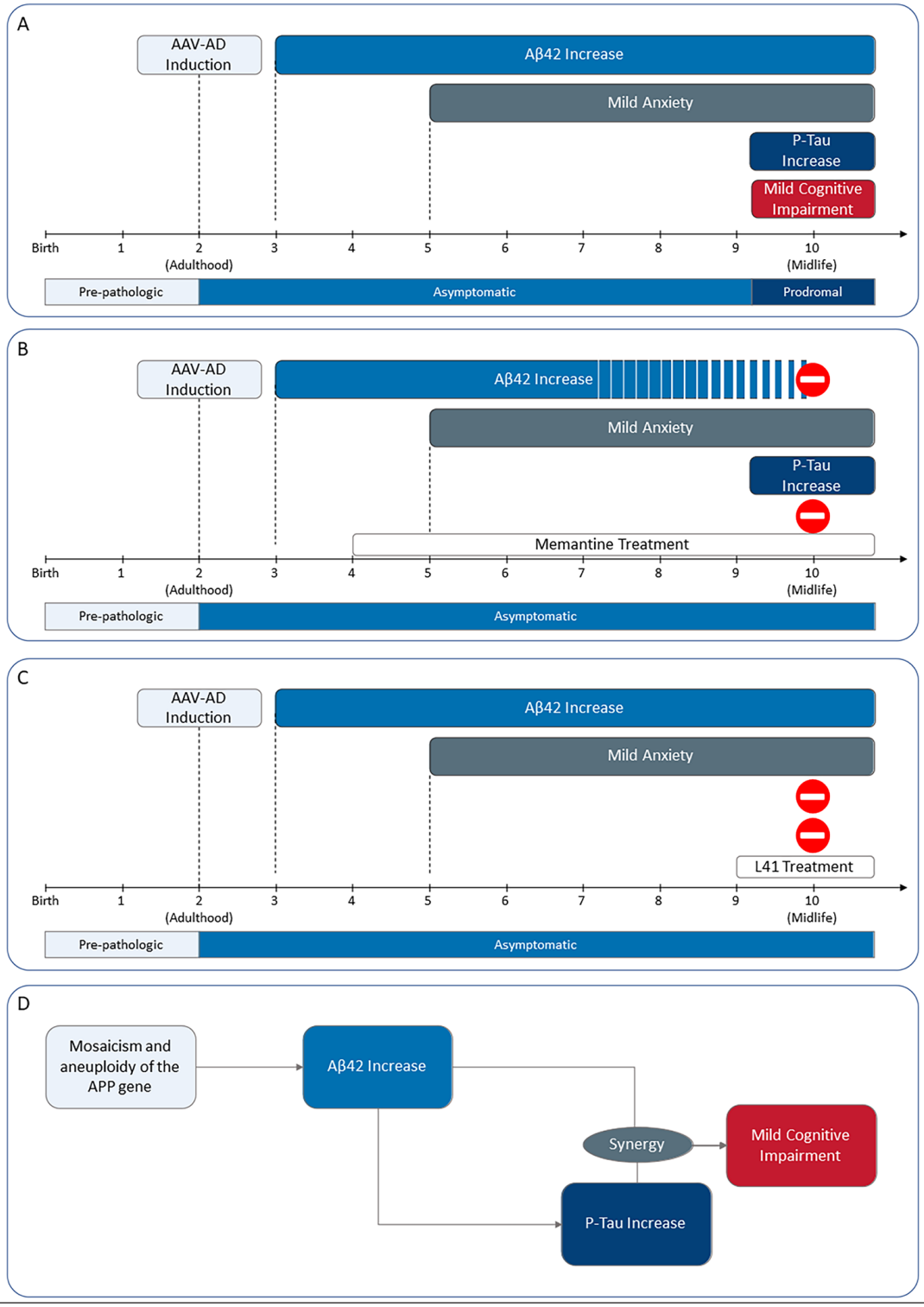

A. Characterization of the AAV-AD rats showed that soluble Aβ production increases progressively in AAV-AD hippocampi following a slow age-dependent process from the adulthood (equivalent to the asymptomatic phase) with mild anxiety as the first behavioral consequence. This progressive amyloidogenic processing of APP then induces hyperphosphorylation of the endogenous tau protein which occurs simultaneously with mild cognitive impairment onset observed with the Morris water maze test (adapted from (12)). B. Administration of memantine at a clinically relevant dose from the asymptomatic stage (4-month-old rats) decreases soluble Aβ42 by promotion of the non-amyloidogenic cleavage of APP, prevents the onset of MCI in 10-month-old AAV-AD rats but fails to reduce hyperphosphorylation of tau. This supports that once P-tau is activated by soluble Aβ42, its level keeps increasing independently. Second, the presence of soluble Aβ42 thus appears to be necessary for the development of MCI (adapted from (15)). C. Administration of Leucettine L41 at the end of the asymptomatic stage (9-month-old rats) reduces hyperphosphorylation of tau, prevents the onset of MCI in 10-month-old AAV-AD rats without a decrease of soluble Aβ42. This support that the presence of soluble P-tau is necessary for the development of MCI (present study). D. These compiled data obtained by studying AAV-AD rats support the hypothesis that the combined presence of both soluble forms of Aβ42 and P-tau is necessary to trigger the shift from asymptomatic to prodromal stage and to induce the onset of cognitive decline observed in Alzheimer's pathology.

previously described (12), 10-month-aged AAV-AD rats show increased phosphorylation levels at numerous tau epitopes including Thr181, Ser422 and Thr212 epitopes (two-way ANOVA, group effect: $p = 0.0001$. Holm-Šídák's multiple comparisons post-hoc test: $p < 0.001$; Fig. 3C). L41-treated AAV-AD rats exhibited a decrease in phosphorylation levels on these epitopes (two-way ANOVA, group effect: $p = 0.0001$. Holm-Šídák's multiple comparisons post-hoc test: $p = 0.003$; Fig. 3C). Note that the decrease in tau phosphorylation level was partial in L41-treated AAV-AD rats and did not reach that of the vehicle-treated control rats (two-way ANOVA, group effect: $p = 0.0001$. Holm-Šídák's multiple comparisons post-hoc test: $p = 0.021$; Fig. 3C). Altogether, these findings confirm that Leucettine L41 treatment reduces hyperphosphorylation of tau without Aβ42 decrease in 10-month-aged AAV-AD rats.

P-tau reduction does not abolish anxiety but prevents mild cognitive impairments

We then evaluated the anxiety level using the open-field task. Vehicle-treated controls, vehicle-treated AAV-AD and L41-treated AAV-AD rats traveled similar distances, showing the absence of motor abnormalities or hyperactivity resulting from AD induction or L41 treatment (one-way ANOVA, $p = 0.887$; vehicle-treated controls: 2.54 ± 0.28 m; vehicle-treated AAV-AD: 2.61 ± 0.19 m; L41-treated AAV-AD: 2.48 ± 0.15 m; data not shown). Nevertheless, vehicle-treated and L41-treated AAV-AD rats spent less time in the center of the open-field apparatus compared to vehicle-treated controls (one-way ANOVA, $p = 0.040$; vehicle-treated controls: 7.80 ± 1.96 s; vehicle-treated AAV-AD: 3.47 ± 1.09 s; L41-treated AAV-AD: 3.39 ± 0.85 s; Tukey's multiple comparisons post-hoc test: $p = 0.069$ and $p = 0.058$, respectively; one outlier was removed in the vehicle-AAV-AD group by the ROUT method (Q=1%) suggesting that Leucettine L41 does not rescue mild anxiety in AAV-AD rats (Fig. 4A).

Morris Water Maze paradigm showed no statistical differences between each learning curves (two-way ANOVA, group effect: $p = 0.956$) as well as during 4 h probe test (two-way ANOVA, group effect: $p = 0.877$, quadrants effect: $p < 0.0001$, Holm-Šídák's multiple comparisons post-hoc test: $p < 0.001$, $p < 0.001$ and $p < 0.001$, respectively) confirming that all rats were able to solve the Morris water maze problem (Fig. 4B and C). During the probe performed 120 hours after the last training session, we observed that vehicle-treated controls rats achieved more distance in the target quadrant compared to the other quadrants. This was not observed with vehicle-treated AAV-AD rats (two-way ANOVA, quadrant effect: $p < 0.001$, Holm-Šídák's multiple comparisons post-hoc test: $p = 0.015$ and $p = 0.309$, respectively) confirming that 10 months-old AAV-AD rats exhibit MCI. Strikingly, Leucettine L41-treated AAV-AD rats swam increased mean distances in the target quadrant (two-way ANOVA, quadrant effect: $p < 0.001$, Holm-Šídák's multiple comparisons post-hoc test: $p = 0.003$) supporting the conclusion that Leucettine L41 treatment prevents accelerated forgetting (Fig. 4D).

Discussion

To date, AD affects 40 million people worldwide and the consensus is to start therapies ideally before the onset of dementia symptoms (22). The first cognitive impairment (mild cognitive impairment) may begin at least 20 years before dementia symptoms (23). While the links between amyloid (amyloid plaques) and tau (tangles) brain lesions and dementia symptoms are now relatively well understood (24), the links between soluble brain forms of Aβ42 and P-tau and the development of MCI remain poorly understood. In this context, we pharmacologically and specifically reduced the levels of P-tau in the AAV-AD rat model without modifying the level of soluble Aβ42. This reduction, initiated 1 month before the onset of MCI, prevented the onset of cognitive decline in Morris Water Maze task. Interestingly, we previously showed that a specific reduction in Aβ42 levels also prevents MCI onset in 10-month-old AAV-AD rats (15). These two studies suggest that the onset of MCI requires the concomitant presence of both cerebral Aβ42 and P-tau. The absence of one of these two soluble forms appears to be sufficient to prevent or at least postpone the onset of initial cognitive decline.

Over the past decade, a shift in the inclusion of patients in clinical trials leads to the enrolment of patients at the prodromal and asymptomatic stages (25, 26). As a consequence, at least three phase 2 or 3 clinical trials have achieved the primary outcome of significantly slowing cognitive decline (6) and one drug (Adulhelm™ aka aducanumab) has been approved by the Food and Drug Administration (FDA), suggesting that the efforts and willingness to treat patients earlier are starting to be efficient. To treat patients earlier and to increase the effectiveness of drugs, it remains important to better understand which forms are responsible for the initial cognitive decline leading to the onset and development of MCI. It is unlikely that the onset of MCI is a consequence of the presence of the aggregated forms of Aβ42 (amyloid plaques) or P-tau (tangles) knowing that threshold of positivity for these lesions is reached in most LOAD patients only at late MCI or dementia stages (8). Indeed, soluble Aβ42 and hyperphosphorylated tau oligomers affect synaptic plasticity before amyloid plaque deposition and the formation of neurofibrillary tangles (27 , 28) and would be responsible for establishing the MCI.

The absence of reliable methods for measuring brain concentrations of these two proteins in living subjects makes it difficult to understand the involvement of Aβ42 and P-tau in the development of MCI in humans. The alternative is to use animal models of LOAD reproducing

the different stages of progression of the pre-dementia pathology. In a previous study (15), we described in AAV-AD rats that pharmacological reduction of brain Aβ42 levels by memantine (without reduction of P-tau levels) prevent the development of MCI. In the presence of tau hyperphosphorylation, the presence of brain Aβ42 is therefore necessary for the conversion from asymptomatic to prodromal stage. In this study, we therefore set out to specifically reduce brain P-tau levels (without reducing Aβ42 levels) to interrogate the involvement of tau hyperphosphorylation in the conversion from asymptomatic to prodromal stage.

To pharmacologically reduce P-tau levels, we used Leucettine L41, a pharmacological inhibitor of the tau kinase DYRK1A (18). Its use has been described *in vitro* to reduce tau protein phosphorylation (19) without reducing Aβ42 levels *in vivo* (20). Thus, administration of Leucettine L41 specifically reduced tau phosphorylation levels without reducing Aβ42 levels in the AAV-AD model. The consequence of this reduction prevented the onset of MCI but did not abolish the mild anxiety. In the presence of increased Aβ42 levels, tau hyperphosphorylation is therefore necessary for the conversion from asymptomatic stage to MCI stage.

Combining the results of the Aβ42 specific reduction study (15) and the results of this study, we confirm the following hypothesis to explain MCI conversion: the initial event is an increase in brain Aβ42 concentration, which will lead to a secondary increase in tau protein phosphorylation. The combined presence of these two soluble forms (obviously as oligomers) will lead to the onset of cognitive decline and thus allow a conversion from asymptomatic to MCI stage. Inhibition of one or other of these pathological pathways abolishes the synergy and thus prevents the transition from asymptomatic to prodromal stage (Fig. 5). Further studies will be needed to determine whether this prevention is maintained over time or whether the maintained pathology could act on its own and lead to the onset of similar or different subsequent cognitive decline such as Suspected Non-Alzheimer disease Pathophysiology (SNAP) (29).

Tauopathies represent more than 20 neurodegenerative diseases, including AD, FTD and Pick's disease. Thereby, the need of drugs reducing the level of phosphorylated-and/or aggregated-tau is essential. A few antibodies and vaccines (such as JNJ-63733657 (NCT04619420), BIIB080 (NCT03186989), Tilavonemab (NCT02880956), Zagotenemab (NCT03019536), ACI-35 (NCT04445831) or Semorinemab (NCT03289143)), are already tested in secondary prevention clinical trials (25) and some of these clinical trials were recently discussed at the Clinical Trials on Alzheimer's Disease (CTAD) meeting in November 2021 in Boston (30), i.e. a few weeks before the publication of this manuscript. Among what was discussed, different IgG4 antibodies binding the N-terminal domain of tau exerted different and even opposite effects in three different Phase 2 trials. Semorinemab (Genentech, AC Immune) slowed cognitive decline on Alzheimer's Disease Assessment Scale-cognitive subscale (ADAS-Cog) while Tilavonemab (AbbVie) didn't show any improvement and while Gosuranemab (Biogen) worsened it. This is just the beginning of tau immunotherapy and these clinical trials will certainly bring crucial insights. Despite the fact that monoclonal antibodies can engage the target in both parenchyma and CSF and hopefully reduce seeding and spreading, tau phosphorylation and aggregation start inside the neurons. Thereby strategies targeting tau intracellularly and using for example antisense oligonucleotides (ASOs) or small molecules are just as decisive.

Full results of these studies are still pending. However, limitations in patient inclusion and biochemical readouts will anyway complicate the achievement of indisputable clinical results. The lack of reliable methods to measure brain concentrations of soluble P-tau in living subjects makes it difficult to confirm the target engagement of these drugs at the brain level. Although technical improvements in plasma biomarkers, including P-tau *per se*, have been recently described (31), the threshold for positivity of this marker is surely not reached before late MCI or dementia in most cases (8), which limits the determination of the optimal therapeutic window for drugs in development. The lack of reliable diagnostic tests also reduces the possibility of including patients from the asymptomatic stage. It is therefore urgent, in parallel with the development of anti-tau molecules, to develop diagnostic methods for pre-dementia Alzheimer's (from the asymptomatic phase) or imaging/biochemical methods to quantify the brain level of P-tau before the formation of tangles. The combined analysis of animal models and complex datasets comprising multiple clinical and biological variables repeated over time could, with the help of artificial intelligence, potentially accelerate the discovery and validation of new biomarkers of Alzheimer's pre-dementia (32).

To summarize, our data provide information about the synergy between Aβ42 and P-tau leading to MCI onset in AAV-AD rats. They also argue that secondary prevention by administration of anti-amyloid and anti-P-tau drugs, used alone or in combination, could, if prescribed during the asymptomatic phase, prevent or postpone the onset of the first MCI cognitive decline. Nonetheless, the development of suitable diagnosis will be required to efficiently validate these therapeutic strategies in preventive clinical trials.

Acknowledgement: We thank Noëlle Dufour, and Gwenaëlle Auregan for their help in producing the viral vectors, Gaëlle Dufayet-Chaffaud for her help in the biochemical analyses, and Yvette Akwa for advice on animal behaviour.

Funding: This work was supported by the DIM Biotherapies, the Région Ile-de-France, IDEX Paris Saclay, INSERM Transfert, CEA "Technologie Pour la Santé" and by a grant from "Investissement d'Avenir—ANR-11-INBS-0011"—NeurATRIS: A Translational Research Infrastructure for Biotherapies in Neurosciences. This research was also supported by grants from the "Fondation Jérôme Lejeune" (LM), the "Agence Nationale pour la Recherche (ANR)" (DYRK-DOWN) (LM, YH), the

"Fonds Unique Interministériel" (FUI) PHARMASEA and TRIAD (LM) projects, and an FP7-KBBE-2012 grant (BlueGenics). This project has received funding from the European Union's Horizon 2020 research and innovation program under grant agreement No 848077 (GO-DS21). This reflects only the authors' view and the European Commission is not responsible for any use that may be made of the information it contains.

Authors' Contributions: B.S., M.A., M.F.L., N.J., L.M. and J.B. carried out the design of the study and wrote the manuscript. B.S., M.A., Y.Y., M.F.L., N.S.O., E.R., and J.B. performed the biochemical, behavioral, and statistical analyses, M.F.L., N.S.O., Y.Y. participated in the biochemical analyses and helped to draft the manuscript. N.C. read the manuscript. All authors read and approved the final manuscript.

Conflict of interest: J.B. is co-founder of AgenT SAS. J.B. and B.S. are employees of AgenT SAS. L.M. is an inventor on the Leucettine patent.

Ethical standards: All experiments were conducted in accordance with the ethical standards of French and European regulations (European Communities Council Directive 2010/63/EU, authorization number APAFIS#4449-2016031012491697).

References

1. Masters CL, Bateman R, Blennow K, Rowe CC, Sperling RA, Cummings JL. Alzheimer's disease. Nat Rev Dis Primers. 2015;1:15056. https://dx.doi.org/10.1038/nrdp.2015.56.
2. Hardy J, Selkoe DJ. The amyloid hypothesis of Alzheimer's disease: progress and problems on the road to therapeutics. Science. 2002;297(5580):353-6. https://dx.doi.org/10.1126/science.1072994.
3. Grundke-Iqbal I, Iqbal K, Quinlan M, Tung YC, Zaidi MS, Wisniewski HM. Microtubule-associated protein tau. A component of Alzheimer paired helical filaments. J Biol Chem. 1986;261(13):6084-9. https://www.ncbi.nlm.nih.gov/pubmed/3084478.
4. Aisen PS, Cummings J, Jack CR, Jr., et al. On the path to 2025: understanding the Alzheimer's disease continuum. Alzheimers Res Ther. 2017;9(1):60. https://dx.doi.org/10.1186/s13195-017-0283-5.
5. Lafirdeen ASM, Cognat E, Sabia S, et al. Biomarker profiles of Alzheimer's disease and dynamic of the association between cerebrospinal fluid levels of beta-amyloid peptide and tau. PLoS One. 2019;14(5):e0217026. https://dx.doi.org/10.1371/journal.pone.0217026.
6. Tolar M, Abushakra S, Hey JA, Porsteinsson A, Sabbagh M. Aducanumab, gantenerumab, BAN2401, and ALZ-801-the first wave of amyloid-targeting drugs for Alzheimer's disease with potential for near term approval. Alzheimers Res Ther. 2020;12(1):95. https://dx.doi.org/10.1186/s13195-020-00663-w.
7. Petersen RC, Caracciolo B, Brayne C, Gauthier S, Jelic V, Fratiglioni L. Mild cognitive impairment: a concept in evolution. J Intern Med. 2014;275(3):214-28. https://dx.doi.org/10.1111/joim.12190.
8. Allegri RF, Chrem Mendez P, Calandri I, et al. Prognostic value of ATN Alzheimer biomarkers: 60-month follow-up results from the Argentine Alzheimer's Disease Neuroimaging Initiative. Alzheimers Dement (Amst). 2020;12(1):e12026. https://dx.doi.org/10.1002/dad2.12026.
9. Morris JC. The Clinical Dementia Rating (CDR): current version and scoring rules. Neurology. 1993;43(11):2412-4. https://dx.doi.org/10.1212/wnl.43.11.2412-a.
10. Cline EN, Bicca MA, Viola KL, Klein WL. The Amyloid-beta Oligomer Hypothesis: Beginning of the Third Decade. J Alzheimers Dis. 2018;64(s1):S567-S610. https://dx.doi.org/10.3233/JAD-179941.
11. Mufson EJ, Ward S, Binder L. Prefibrillar tau oligomers in mild cognitive impairment and Alzheimer's disease. Neurodegener Dis. 2014;13(2-3):151-3. https://dx.doi.org/10.1159/000353687.
12. Audrain M, Souchet B, Alves S, et al. betaAPP Processing Drives Gradual Tau Pathology in an Age-Dependent Amyloid Rat Model of Alzheimer's Disease. Cereb Cortex. 2018;28(11):3976-93. https://dx.doi.org/10.1093/cercor/bhx260.
13. Bushman DM, Kaeser GE, Siddoway B, et al. Genomic mosaicism with increased amyloid precursor protein (APP) gene copy number in single neurons from sporadic Alzheimer's disease brains. Elife. 2015;4. https://dx.doi.org/10.7554/eLife.05116.
14. Lee MH, Siddoway B, Kaeser GE, et al. Somatic APP gene recombination in Alzheimer's disease and normal neurons. Nature. 2018;563(7733):639-45. https://dx.doi.org/10.1038/s41586-018-0718-6.
15. Souchet B., Audrain M., Alves S., et al.. Evaluation of Memantine in AAV-AD Rat: A Model of Late-Onset Alzheimer's Disease Predementia. 2021.Journal of Prevention of Alzheimer's Disease. https://dx.doi.org/10.14283/jpad.2021.67.
16. Ryoo SR, Jeong HK, Radnaabazar C, et al. DYRK1A-mediated hyperphosphorylation of Tau. A functional link between Down syndrome and Alzheimer disease. J Biol Chem. 2007;282(48):34850-7. https://dx.doi.org/10.1074/jbc.M707358200.
17. Debdab M, Carreaux F, Renault S, et al. Leucettines, a class of potent inhibitors of cdc2-like kinases and dual specificity, tyrosine phosphorylation regulated kinases derived from the marine sponge leucettamine B: modulation of alternative pre-RNA splicing. J Med Chem. 2011;54(12):4172-86. https://dx.doi.org/10.1021/jm200274d.
18. Tahtouh T, Elkins JM, Filippakopoulos P, et al. Selectivity, cocrystal structures, and neuroprotective properties of leucettines, a family of protein kinase inhibitors derived from the marine sponge alkaloid leucettamine B. J Med Chem. 2012;55(21):9312-30. https://dx.doi.org/10.1021/jm301034u.
19. Tahtouh T, Durieu, E., Villiers, B., et al. Structure/activity relationship in the Leucettine family of kinase inhibitors. . J Med Chem. 2021;in press.
20. Souchet B, Audrain M, Billard JM, et al. Inhibition of DYRK1A proteolysis modifies its kinase specificity and rescues Alzheimer phenotype in APP/PS1 mice. Acta Neuropathol Commun. 2019;7(1):46. https://dx.doi.org/10.1186/s40478-019-0678-6.
21. Vasta JD, Corona CR, Wilkinson J, et al. Quantitative, Wide-Spectrum Kinase Profiling in Live Cells for Assessing the Effect of Cellular ATP on Target Engagement. Cell Chem Biol. 2018;25(2):206-14 e11. https://dx.doi.org/10.1016/j.chembiol.2017.10.010.
22. McDade E, Bateman RJ. Stop Alzheimer's before it starts. Nature. 2017;547(7662):153-5. https://dx.doi.org/10.1038/547153a.
23. Rajan KB, Wilson RS, Weuve J, Barnes LL, Evans DA. Cognitive impairment 18 years before clinical diagnosis of Alzheimer disease dementia. Neurology. 2015;85(10):898-904. https://dx.doi.org/10.1212/WNL.0000000000001774.
24. DeTure MA, Dickson DW. The neuropathological diagnosis of Alzheimer's disease. Mol Neurodegener. 2019;14(1):32. https://dx.doi.org/10.1186/s13024-019-0333-5.
25. Cummings J, Lee G, Zhong K, Fonseca J, Taghva K. Alzheimer's disease drug development pipeline: 2021. Alzheimers Dement (N Y). 2021;7(1):e12179. https://dx.doi.org/10.1002/trc2.12179.
26. Cummings J, Morstorf T, Lee G. Alzheimer's drug-development pipeline: 2016. Alzheimers Dement (N Y). 2016;2(4):222-32. https://dx.doi.org/10.1016/j.trci.2016.07.001.
27. Sengupta U, Nilson AN, Kayed R. The Role of Amyloid-beta Oligomers in Toxicity, Propagation, and Immunotherapy. EBioMedicine. 2016;6:42-9. https://dx.doi.org/10.1016/j.ebiom.2016.03.035.
28. Berger Z, Roder H, Hanna A, et al. Accumulation of pathological tau species and memory loss in a conditional model of tauopathy. J Neurosci. 2007;27(14):3650-62. https://dx.doi.org/10.1523/JNEUROSCI.0587-07.2007.
29. Jack CR, Jr., Knopman DS, Chetelat G, et al. Suspected non-Alzheimer disease pathophysiology--concept and controversy. Nat Rev Neurol. 2016;12(2):117-24. https://dx.doi.org/10.1038/nrneurol.2015.251.
30. Abstract: Symposia, Conferences, Oral communications: 14th Clinical Trials on Alzheimer's Disease (CTAD) November 9-12, 2021. J Prev Alzheimers Dis. 2021;8(S1):S2-S72. https://dx.doi.org/10.14283/jpad.2021.57.
31. Zou K, Abdullah M, Michikawa M. Current Biomarkers for Alzheimer's Disease: From CSF to Blood. J Pers Med. 2020;10(3). https://dx.doi.org/10.3390/jpm10030085.
32. Ader I, Penicaud L, Andrieu S, et al. Healthy Aging Biomarkers: The INSPIRE's Contribution. J Frailty Aging. 2021;10(4):313-9. https://dx.doi.org/10.14283/jfa.2021.15.

How to cite this article: B. Souchet, M. Audrain, Y. Gu, et al. Cerebral Phospho-Tau Acts Synergistically with Soluble Aβ42 Leading to Mild Cognitive Impairment in AAV-AD Rats. J Prev Alz Dis 2022; http://dx.doi.org/10.14283/jpad.2022.18

View publication stats